Coherent structures in boundary layers of Rayleigh-Bénard convection

T. Haramina and A. Tilgner
Institute of Geophysics, University of Göttingen, Herzberger Landstrasse 180, 37075 Göttingen, Germany
(Received 15 October 2003; revised manuscript received 9 January 2004; published 21 May 2004)

A coherent structure is revealed experimentally by a dyeing technique in the boundary layer of Rayleigh-Bénard convection in water. Dye accumulates in streaks aligned with the mean flow. Possible mechanisms for the formation of these streaks are discussed.

DOI: 10.1103/PhysRevE.69.056306 PACS number(s): 47.27.Te, 44.25.+f

Fluctuations in a turbulent flow are usually classified in two broad classes. There are those fluctuations which are disorganized enough so that we have to unspecifically describe them as "turbulent." But one sometimes finds recognizable patterns, such as groups of vortices, or vortices of special shape, which appear repeatedly. These organized recurrent patterns are "coherent structures" which are distinguished from the turbulent background. Coherent structures have been studied particularly well in turbulent boundary layers, where an understanding of these structures contributes to our ability to control flows [1]. More fundamentally, coherent structures are a curiosity in themselves because they exist in defiance of a turbulent environment. If one wants to give a more informative description than just saying that a flow is turbulent, the next step consists in enumerating its coherent structures. The identification of coherent structures is thus important because it reveals some order in otherwise featureless and unruly dynamics.

Thermal convection is an omnipresent phenomenon in engineering applications, astrophysics, and geophysics. The archetypal buoyant coherent structure is the plume. Its characteristics have been studied in detail (see, for example, Ref. [2]) and plumes have remained for a long time the only known coherent structure of turbulent convection. Zocchi *et al.* [3] later identified "swirls" and waves riding the thermal boundary layer. Here, we add a coherent structure in the boundary layers of Rayleigh-Bénard convection. A dye technique to be described below reveals accumulation of dye in streaks exactly as it would be produced by pairs of streamwise counterrotating vortices.

A cubic cell of size 20 cm filled with water was used in our visualization experiments. The side walls were made of 10 mm thick plexyglas whereas the top and bottom plates were 10 mm thick silver coated copper plates. Electrical heaters were attached to the bottom plate and the temperature of the top plate was regulated by circulating water from a thermostat through pipes welded to the top plate. The plate temperatures were uniform in space and time to better than 0.1 K. The temperatures of the two plates differed by approximately 10 K and were adjusted such that the bulk temperature in the cell was near the room temperature in the laboratory. The data below are for a Prandtl number Pr of 6.7 and a Rayleigh number Ra of 1.3×10^9. The entire setup is nearly identical to the one used in Ref. [4]. Measurements of velocity and temperature profiles in the new cell were consistent with those in Ref. [4]. A single convection roll exists in the cell such that the average flow near the plates is directed diagonally across the plates.

Flow structures were visualized with the thymol blue technique [5]. The *p*H-indicator thymol blue was dissolved at a concentration of around 10^{-4} per weight in the water. The solution was titrated with HCl and NaOH just to the acid side of the end point of the indicator so that the solution was orange yellow. The bottom plate of the cell was used as cathode and a wire sticking into the cell as anode. If a current is sent through the cell, H^+ ions are drawn towards the bottom plate where they react to H_2 which leads to a local increase of the *p*H. If the increase is large enough, the liquid appears dark blue. Once a darkened drop of fluid gets carried away from the electrode by the flow, it loses through diffusion its *p*H contrast with the environment and turns orange yellow again. In our experiments, the voltage applied between the electrodes was typically 3 V so that the production of blue dye was too small to be visible everywhere. Only higher than average concentrations of blue dye appeared dark.

The basic observation is that dark fluid accumulates in streaks aligned with the mean wind (Fig. 1). Streaks appear in groups within which there is an apparent periodicity. The streaks are advected by the mean circulation and lift off the plate when they approach a sidewall. The number of visible streaks increases with downstream distance and the first ones appear shortly before they reach the diagonal of the bottom plate perpendicular to the mean flow (the line *AB* in Fig. 1).

The appearance of streaks indicates that blue dye is swept together by the flow. The convergence of the flow towards the lines where streaks form requires that fluid rises above the streaks and that downwellings exist in between streaks. A

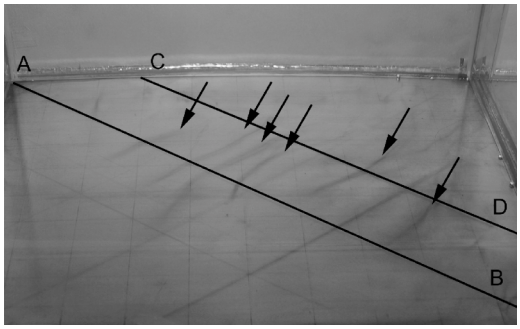

FIG. 1. View of the bottom plate. The point labeled *A* is one corner of the plate, and the line through *A* and *C* is one side of the plate. The mean flow is from the near left to the far right corner. A few dye streaks are marked with arrows.

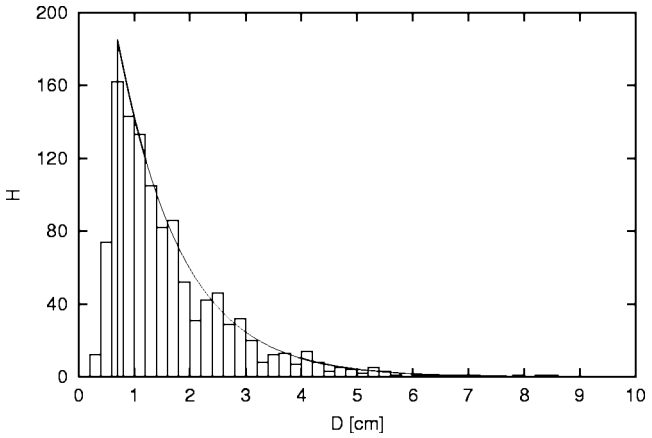

FIG. 2. The bar chart is a histogram of the streak separation D measured on the line CD in Fig. 1. 134 photographs showing a total of 1277 streaks were used. The continuous line is $H(D)$ given by Eq. (4) for $\Delta D=0.2$ mm, $\delta=0.6$ cm, and $p=0.82$.

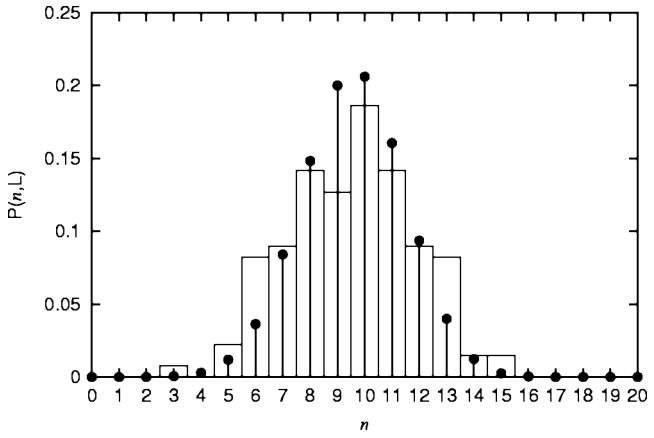

FIG. 3. The bar chart is the probability distribution for the number of streaks n visible in any one photograph on the line CD for the same data as in Fig. 2. The dots give $P(n,L)$ [Eqs. (5) and (6)] for $L=19.8$ cm, $\delta=0.6$ cm, and $p=0.82$.

pattern of closed streamlines producing a single streak would be a pair of counterrotating vortices superposed on, and aligned with, the mean flow.

In these experiments, the solution must be carefully titrated and the voltage chosen as small as possible so that the observed dye is as close as possible to the plate. At higher voltages, the blue dye still appears in streaks, but much of it is separated from the plate and probes regions in which the flow is clearly three dimensional instead of nearly parallel to the boundary.

In order to acquire quantitative information about the streak spacing, pictures of the cell have been taken with a 5 megapixel charge-coupled device camera. One photograph has been taken every 60 s so that consecutive pictures are statistically independent. A grid of lines spaced by 2 cm was drawn with a graphite pencil on the bottom plate for calibration of the pictures. We determined manually for each picture the positions at which streaks cross either the main diagonal perpendicular to the mean flow (AB in Fig. 1), or where they cross the diagonal CD (see Fig. 1) which is a line joining two points on the edges of the plate which are 4 cm away from the corners in the downstream direction (this diagonal has a length of 19.8 cm).

Streaks are uniformly distributed over AB or CD. The streaks thus are not related to possible defects in the bottom plate. The histogram of streak separations on the other hand has a pronounced peak around 0.7 cm (Fig. 2). Less extensive statistics for Ra in between 5×10^8 and 4×10^9, and with Pr ranging from 3.6 to 6.7 have shown that the position of this peak does not vary by more than 20 % in the range of parameters investigated. The histogram of the number of streaks crossing CD at any instant in time is shown in Fig. 3. The average number increases from 6.3 to 9.5 in going from AB to CD.

We will now discuss different mechanisms which might lead to streak formation. The peak in the histogram of streak spacings is a hint at an underlying periodicity. Periodic streamwise vortices are well known from isothermal momentum boundary layers where they have a periodicity length of about 100 wall units [one "wall unit" is $\nu^{1/2}(dU/dz)^{-1/2}$ where ν is the viscosity and dU/dz the velocity gradient at the wall]. However, these structures occur at much higher Reynolds numbers than we have in our convection cell. Based on the advection velocity at the edge of the viscous boundary layer and the thickness of that layer, the Reynolds number is less than 30. Not surprisingly, 100 wall units correspond to 8.5 cm in the convection cell which is much too large to explain the peak in the histogram of streak separations.

There is a theory successfully predicting the streamwise vortices in isothermal boundary layers which is based on the observation that the linearized stability problem is not normal so that large transient growth can occur. We extended this theory and the calculations in Refs. [6] and [7] by including a linear temperature profile and the buoyancy force. At the parameters relevant for the experiment, no significant transient amplification occurs, so that this mechanism must be excluded, too.

The next candidate is linear instability. The thermal boundary layer is notoriously stable with respect to convection within that layer. However, the hot fluid near the bottom plate underneath the cooler bulk of the fluid is Rayleigh-Taylor unstable. Temperature and velocity in the boundary layers are of course fluctuating in time and the actual profiles are shaped by turbulent transport. We nonetheless solved the linear stability problem for this layering using as basic state the time averaged velocity and temperature profiles measured experimentally in Ref. [4] in order to find a possible connection between streak formation and a Rayleigh-Taylor instability.

The linear stability problem is described by the equations

$$\partial_t \boldsymbol{v} + (\boldsymbol{v}\cdot\boldsymbol{\nabla})\boldsymbol{U} + (\boldsymbol{U}\cdot\boldsymbol{\nabla})\boldsymbol{v} = -\frac{1}{\rho}\boldsymbol{\nabla} p + \nu\boldsymbol{\nabla}^2\boldsymbol{v} - \boldsymbol{g}\alpha T, \quad (1)$$

$$\nabla\cdot\boldsymbol{v} = 0, \quad (2)$$

$$\partial_t T + \boldsymbol{v}\cdot\boldsymbol{\nabla} T_0 + \boldsymbol{U}\cdot\boldsymbol{\nabla} T = \kappa\boldsymbol{\nabla}^2 T. \quad (3)$$

p is the pressure; $\boldsymbol{g}$ the gravitational acceleration, and ρ, ν, α, and κ are the density, viscosity, thermal expansion coeffi-

cient, and thermal diffusivity, respectively. A Cartesian coordinate system (x,y,z) is used such that the z axis points upwards and the bottom plate is located at $z=0$. $\boldsymbol{U}(z)$ and $T_0(z)$ are the undisturbed profiles of velocity and temperature. The total velocity is $\boldsymbol{v}(x,y,z,t)+\boldsymbol{U}(z)$ and the total temperature is $T(x,y,z,t)+T_0(z)$. The problem is linear in $\boldsymbol{v}$ and T with coefficients independent of x, y, and t so that the dependence of $\boldsymbol{v}$ and T on these variables must be of the form $e^{\sigma t}e^{i(k_x x+k_y y)}$. Three ordinary differential equation in z are obtained from $\boldsymbol{z}\cdot\boldsymbol{\nabla}\times(1)$, $\boldsymbol{z}\cdot\boldsymbol{\nabla}\times\boldsymbol{\nabla}\times(1)$ and (3) which pose for any fixed wave numbers k_x and k_y an eigenvalue problem with the growth rate σ as eigenvalue. The boundary conditions used to complete the eigenvalue problem are $\boldsymbol{v}=0$ and $T=0$ at $z=0$ and $z=z_{max}$, where z_{max} is an arbitrarily chosen upper boundary of the computational domain. The eigenvalues are computed numerically with a Chebychev spectral method. With $\boldsymbol{U}$ and T_0 taken from Ref. [4], the x-axis chosen parallel to $\boldsymbol{U}$, and with the material properties of water, one finds that the most unstable eigenmode becomes independent of the choice of z_{max} for $z_{max}>6$ mm. The most unstable mode is also virtually unaffected by the fact that $\boldsymbol{U}\neq 0$. $\boldsymbol{U}$ is apparently too small to play a significant role except that it gives a preference to longitudinal over transverse vortices. The most unstable mode is characterized by $k_x=0$, $2\pi/k_y=6.5$ mm, and $\sigma=0.54\ \mathrm{s}^{-1}$. For comparison, note that the thicknesses of the temperature and velocity boundary layers are 1.9 mm, and 3.8 mm, respectively. The cell used here is somewhat bigger than the cell used in Ref. [4]. Correcting for the size difference, a wavelength of 7.2 mm is obtained for the new cell.

The computed growth rate, combined with the advection velocity, implies that there should be at least seven times as many visible streaks on *CD* than on *AB*. In reality, this factor is approximately 1.5. The observed structures must thus be far beyond the stage of exponential growth if they result from a Rayleigh-Taylor instability.

Up to now, we have interpreted the peak in the histogram of separations as the result of a periodicity. We now show how a complementary point of view explains the shape of the histograms in Figs. 2 and 3. Assume that the streaks are signatures of isolated pairs of vortices. Two such structures cannot come too close to each other because they need room from where to collect fluid. If we suppose that streaks are mutually independent apart from this excluded volume, we can compute histograms and compare them to experimental data.

Consider a diagonal of length L and denote by x the distance along the diagonal from one of its end points. For simplicity, we will assume that all structures have the same lateral size δ. If a streak at location x is created by a pair of vortices, the streak is surrounded by a vortex of size $\delta/2$ on each side and the structure extends from $x-\delta/2$ to $x+\delta/2$. The point at $x-\delta/2$ will be called the "left edge" of the coherent structure. Denote by pdx the probability to find a left edge in an interval dx. The probability to find a segment of length l free of left edges is then e^{-pl}.

In order to compute the experimental histogram, we have to take into account the finite length of the diagonal. If two streaks are separated by a distance D, the leftmost of the two streaks must have a left edge at a distance of at most $L-D-\delta$ from the left end of the diagonal so that the second streak still fits onto the diagonal. Left edges are equally distributed in the interval $[0,L-\delta]$. The probability to find two streaks separated by a distance between D and $D+dD$ is equal to the probability that a streak picked at random is in the interval $[0,L-D-\delta]$, multiplied by the probability not to find a left edge over a distance $D-\delta$, multiplied by the probability to find one in the following interval dD, which is all taken together equal to $(L-D-\delta)/(L-\delta)e^{-p(D-\delta)}p\ dD$. A histogram of streak separations $H(D)$ with bins of size ΔD constructed from N_p photographs with on average N visible streaks is given by

$$H(D)=\begin{cases}\dfrac{L-D-\delta}{L-\delta}e^{-p(D-\delta)}p\,\Delta D\,N_pN, & \delta<D<L-\delta\\ 0, \quad \text{otherwise}.\end{cases} \tag{4}$$

This expression will be used to fit the histogram in Fig. 2. Let us now turn to Fig. 3. Denote by $P(n,l)$ the probability to find n streaks at any given time in an interval of length l. $P(n,l)$ can be computed recursively as follows:

$$P(0,l)=\begin{cases}1, & l<\delta\\ e^{-p(l-\delta)}, & l\geqslant\delta,\end{cases} \tag{5}$$

and for $n>0$:

$$P(n,l)=\begin{cases}0, & l<n\delta\\ \displaystyle\int_0^{l-\delta}dx e^{-px}pP(n-1,l-x-\delta), & l\geqslant n\delta.\end{cases} \tag{6}$$

The last line represents the probability not to find a left edge of a structure up to location x, multiplied by the probability to find one immediately afterwards, multiplied by the probability to find $n-1$ further streaks in the remaining interval, integrated over all x in which the left edge of a structure can be located.

A disadvantage of this simple model is that $H(D)$ is strictly zero for $D<\delta$ which poorly represents the histogram of streak separations at small D. A more complete model would allow for a distribution of δ which we do not do here because it inordinately increases the number of adjustable parameters. Instead, we take for δ approximately the D at which the experimental histogram is maximum and adjust p so that $P(n,L)$ fits Fig. 3 as well as possible. We then plug p into the expression for $H(D)$ in (4) and verify that it acceptably fits Fig. 2. The results of this procedure are shown in Figs. 2 and 3.

It is seen that it is not necessary to assume a periodicity in order to reproduce a histogram of streak separations with a peak. In fact, within the limits of the statistical noise on the experimental side and the restriction to a unique δ in the model, the experimental data are satisfactorily fitted by the assumption of mutually independent coherent structures.

We have also seen above that the size of these structures is close to the periodicity length of the Rayleigh-Taylor instability of the thermal boundary layer. Further experiments

are necessary in order to decide whether the streaks arise from pairs of rolls generated by such an instability. For example, a variation of Ra over several decades will show whether the linear stability analysis presented here reproduces the most probable streak spacing at all Ra. As long as the Reynolds number is small in the boundary layers, the thickness of the boundary layer is the only length scale entering the mathematical problem, so that the most probable streak spacing should scale as Nu^{-1}, where Nu is the Nusselt number.

In summary, we have demonstrated the existence of a hitherto unnoticed coherent structure in the boundary layers of Rayleigh-Bénard convection. This structure reveals itself through dye accumulation in streaks aligned with the mean wind which keep a characteristic separation from each other. The dye pattern could be produced by pairs of counterrotating vortices, but no direct visualization of the velocity field has been made. Streamwise vortices are well known from isothermal boundary layers, but the mechanism of formation of these vortices must be different here because of the low Reynolds number of the boundary layer flow. The statistics of the streaks are consistent with the notion that they are created by coherent structures which are independent of each other except for an excluded volume effect.

This work was supported by the "Deutsche Forschungsgemeinschaft."

[1] S. Robinson, Annu. Rev. Fluid Mech. **23**, 601 (1991).
[2] G. Taylor, Proc. R. Soc. London, Ser. A **201**, 175 (1950).
[3] G. Zocchi, E. Moses, and A. Libchaber, Physica A **166**, 387 (1990).
[4] A. Tilgner, A. Belmonte, and A. Libchaber, Phys. Rev. E **47**, R2253 (1993).
[5] D. Baker, J. Fluid Mech. **26**, 573 (1966).
[6] S. Reddy and D. Henningson, J. Fluid Mech. **252**, 209 (1993).
[7] K. Butler and B. Farrell, Phys. Fluids A **4**, 1637 (1992).